IDENTIFYING NOVEL MUTANTS WITH INCREASED SUSCEPTIBILITY TO H_2O_2 AND REDUCED VIRULENCE IN *BACILLUS ANTHRACIS*

by

Luke Todd Hamilton

Submitted in partial fulfillment of the

requirements for Departmental Honors in

the Department of Biology

Texas Christian University

Fort Worth, Texas

May 8, 2023

IDENTIFYING NOVEL MUTANTS WITH INCREASED SUSCEPTIBILITY TO H_2O_2 AND REDUCED VIRULENCE IN *BACILLUS ANTHRACIS*

Project Approved:

Supervising Professor: Shauna McGillivray, Ph.D.

Department of Biology

Giridhar Akkaraju, Ph.D.

Department of Biology

Jada Willis, Ph.D.

Department of Nutritional Sciences

ABSTRACT

Bacillus anthracis is a gram-positive bacterial pathogen that causes the deadly infectious disease anthrax. *B. anthracis* contains over 5,000 chromosomal genes, and we believe there are unidentified chromosomal genes important for virulence. To identify novel virulence genes, our lab constructed a transposon mutant library with random disruptions in the *B. anthracis* Sterne genome and screened for virulence-associated phenotypes. Previous screens successfully identified two novel virulence genes*, clpX* and *yceGH,* using this library. In this screen, we used H_2O_2, a reactive oxygen species involved in innate immune defense, and screened around 1000 mutants. We obtained three mutants that were susceptible to hydrogen peroxide *in vitro*: 11F11, LV1, and LV2. To determine whether they also had phenotypes *in vivo*, we infected *Galleria mellonella* to study their virulence in an invertebrate animal infection model. LV2 showed reduced virulence in the *in vivo* survival assay, and all three mutants showed reduced virulence in the *in vivo* competition assay. I have determined the site of the transposon insertion in 11F11 and LV1, and the transposon has inserted in the genes for catalase and a collagenase-like protein, respectively. I attempted to create an independent insertional mutation in LV1 to confirm that the observed phenotypes are linked to the disruption of the collagenase-like protein; however homologous recombination has not been successful. Future directions include creating a complementation plasmid for LV1 and determining the insertion site of LV2. The findings of this research could be used as potential therapeutic drug targets and will offer insight into the mechanisms that *B. anthracis* uses for its pathogenesis.

ACKNOWLEDGEMENTS

I would like to give a special thank you to Dr. Shauna McGillivray, my research mentor and advisor during my time at TCU. She has provided me with an avenue to expand on what I have learned in the classroom and apply it in a hands-on manner in the lab. My interest in microbiology and research has blossomed from watching her enthusiastically teach one of her greatest passions, demonstrate new protocols and techniques to me, and challenging me to problem solve and troubleshoot my own adversity I face with my assays. She has been extremely supportive of every endeavor I have set my eyes on and has provided me with countless opportunities through state-wide conferences to grow as a scientist and person. I would also like to thank my committee members, Dr. Giri Akkaraju and Dr. Jada Willis, for their support of my research project and encouragement in the classroom. Dr. Giri Akkaraju, thank you for letting me bombard your lab to hangout and use your scale to weigh waxworms! Dr. Jada Willis, thank you for your selflessness and willingness to serve on my committee during your first semester back from maternity leave. Additionally, thank you to the TCU Pre-Health Professions Institute Summer Research Fellowship and TCU Science and Engineering Research Center for your financial support of this project. I also want to thank all members of the McGillivray lab who have made my time in and out of the lab so enjoyable: Victoria Adeleke, Alex Caron, Lauren Klingemann, Bella Kouretas, Zach Rouseau, Kelsey Waite, Michael Delgado, Lilly Wilson, Abi Plylar, Sheridan O'Coyne, Kyle Gallegos, Salina Hona, and Vuong Do. Finally, thank you to my friends and family who have been the backbone of my college experience by supporting and encouraging me throughout all my academic and career endeavors.

TABLE OF CONTENTS

INTRODUCTION

Bacillus anthracis is a gram positive, rod-shaped, spore forming bacterium that causes the deadly infectious disease anthrax. *B. anthracis* can persist for years in the soil as spores when conditions are unfavorable [1]. Once these spores are returned to an environment that is favorable like the tissues of an animal host, the spores germinate and present a threat of becoming systemic in the animal host [2]. If this bacterium is able to successfully kill the host and exhaust its current environment, it can still reside in localized infectious zones, and the remaining *B. anthracis* spores are able to spread to other hosts or remain in the soil for years awaiting the perfect conditions to gain a foothold in the next host [3]. Field studies have confirmed the spread of *B. anthracis* from necrophagous flies to persimmons in Texas [3], and, more recently, the transmission of disease via intravenous injections of contaminated heroin in Europe [4].

Anthrax has a high variability in the severity and route of infection, which can often make it difficult to diagnose and treat. There are four routes of infection: cutaneous, inhalation, gastrointestinal, and injection anthrax. Cutaneous anthrax is the most common and least lethal form of infection [5]. It usually manifests as black eschars with corresponding edema and purplish vesicles on affected areas. The infection is introduced to the host through pathogenic endospores entering subcutaneously through abrasions or exposed cuts in the skin. Approximately 80-90% of these cases resolve without complications [6]. Gastrointestinal anthrax occurs when *B. anthracis* endospores breach the mucosal lining and germinate in the tissue. Ulceration is seen in the mucosal and submucosal lymphatic tissue, and corresponding massive edema and mucosal necrosis is observed at these infected sites [6]. Inhalation anthrax is the most lethal form of anthrax. This anthrax manifests when *B. anthracis* spores are inhaled and

deposited in the alveoli before being phagocytosed and traveling to the lymph nodes where they germinate. If treatment is ineffective, toxemia and bacteremia may ensue, which may progress to death of the host [5]. Injection anthrax is transmitted through intravenous, subcutaneous or intramuscular injection with anthrax-laced, contaminated heroin. Even with medical treatment, the mortality rate is approximately 35% [4]. There are many presumed sources of contamination for how this anthrax-laced heroin started circulating in Europe. One presumed source is an anthrax-contaminated, animal-based cutting agent, another is anthrax-contaminated animal hides that are used to wrap around the drug, and the last is contact with soil containing anthrax spores throughout drug manufacturing and trafficking [4]. Due to the many routes of infection for *B. anthracis* and the higher mortality rates associated with inhalation and injection anthrax, this bacterium has the potential to be used in bioterrorist acts. In 2001, letters laced with anthrax spores were mailed to U.S. politicians through the mail system. 22 individuals contracted anthrax and 5 cases were fatal [7]. Due to the lethal nature of the disease and the potential for its use as a bioweapon, the virulence mechanisms of *B. anthracis* are of high interest.

The *B. anthracis* genome has more than 5000 chromosomal genes and two virulence plasmids, pXO1 and pXO2. pXO1 contains the structural genes that encode the three anthrax toxin proteins: edema factor (EF), lethal factor (LF), and the protective antigen (PA). Together, these three polypeptides combine to form the lethal toxin and edema toxin which interfere with cell signaling in the innate immune system of the host [1]. pXO2 encodes the antiphagocytic polyglutamic capsule which protects the bacterium from being recognized and phagocytosed by the host immune system [1]. The fully virulent strain of *B. anthracis* is the Ames strain, which contains both plasmids. The strain used in our lab, the Sterne strain, lacks the pXO2 plasmid and therefore loses a vital virulence factor important for the pathogenicity of anthrax.

While there is thorough research studying these two plasmids, there is not as much known about the chromosomal genes of *B. anthracis.* However, previous sequencing of the *B. anthracis* genome has noted homology to several potential virulence genes that are yet to be identified [8]. To study the role of the chromosomal genes, Dr. Shauna McGillivray created a transposon mutant library using transposon mutagenesis [9]. This library contains different transposon mutants, each with a transposon DNA sequence inserted randomly in the *B. anthracis* genome. Dr. Shauna McGillivray began screening this library and performed a variety of screens assessing virulence in *Caenorhabditis elegans,* proteolytic activity, and hemolytic activity of these transposon mutants. From this library, the transposon mutants with an interruption in the chromosomal genes *clpX* [9]and *yceGH* [10], respectively, were identified as having decreased virulence.

In order to identify additional novel virulence genes, another undergraduate researcher, Victoria Adeleke, and I began screening this transposon mutant library for increased hydrogen peroxide susceptibility. Hydrogen peroxide is a reactive oxygen species and is often implicated in the mammalian host immune response to pathogens. Transposon mutants selected for in this initial screen were subjected to an *in vivo* assay in the invertebrate animal, *Galleria mellonella,* to see if they exhibited reduced virulence compared to wild-type *B. anthracis*. *G. mellonella* has conserved immune defenses like the production of antimicrobial peptides and reactive oxygen species, which mimics the vertebrate innate immune system. This model has shown its susceptibility to *Staphylococcus aureus, Acinetobacter baumannii, Cryptococcus neoformans,* and *Candida albicans* virulence in previous studies [11-14]. Additionally, this model has been successfully validated as an effective infection model for *B. anthracis* in previous competition and survival assays [15]. If these mutants of interest continue to show a phenotype in these *in*

vivo studies, then I will move forward to determine the insertion site. This will allow us to identify novel, critical virulence genes in *B. anthracis* and give us further insight into the pathogenesis of anthrax.

METHODS

In vitro minimum inhibitory concentration (MIC) screen

B. anthracis transposon mutants from a previously created frozen transposon mutant library [9] were spread across brain and heart infusion media (BHI) kanamycin plates to allow for isolated bacterial colony growth. The following day, isolated colonies were selected and placed into individual wells on a 96-well plate containing 200 µl of BHI kanamycin broth. Wells 1, 2, and 96 were reserved for positive and negative controls. The remaining wells contained the mutants. The 96-well plate was incubated at 37 °C for ~12-15 hours in static conditions. After overnight incubation, one pass of the bacterial cultures was performed by taking 25 µl of the day two overnight culture and adding it to 175 µl of BHI in a new 96-well plate. The day three plate was then incubated at 37 °C for ~12-15 hours in static conditions. On day four, a 0.035% hydrogen peroxide BHI media solution was prepared, and 175 µl of this media solution was added to each well on a new 96-well plate before 25 µl of the day three overnight culture was added. After overnight incubation at 37 °C for ~12-15 hours in static conditions, the optical density (OD) of each bacterial culture was read using an absorbance at 600 nm wavelength on the spectrophotometer.

Large-volume MIC screen

Mutants identified from the initial MIC screen were subjected to a large-volume MIC assay using 5 mL culture tubes instead of the 96-well plate. One colony of each bacterial culture was placed in 1 mL BHI Kan-50 and grown overnight at 37 °C for ~12-15 hours in shaking conditions. The next day for stationary phase testing, the overnight cultures were diluted 1:20 before 100 µl of each bacterial culture was placed in wells with 100 µl of a H_2O_2-BHI solution in each well to achieve a gradient of concentrations ranging from 0% to 0.2% H_2O_2-BHI in a 200 µl final volume. For logarithmic phase testing, we first removed 100 µl of the overnight culture and added it to 3 mL BHI in a 16 mL glass culture tube to grow them up to logarithmic phase. Upon reaching log phase, we performed the 1:20 dilution and then created the gradient of concentrations ranging from 0% to 0.2% H_2O_2-BHI in a 200 µl final volume. After overnight incubation at 37 °C for ~12-15 hours in static conditions, the optical density (OD) of each bacterial culture was read using an absorbance at 600 nm wavelength on the spectrophotometer.

Growth curve protocol

Overnight cultures of wild-type (WT), 4D5, 11F11, LV1, and LV2 were grown at 37 °C for ~12-15 hours. The following day, 100 µl of overnight culture was added to 3 mL of BHI to create day cultures that were incubated at 37 °C for 6 hours. Growth was monitored hourly by checking the optical density (OD) of each bacterial culture using an absorbance at 600 nm wavelength on the spectrophotometer.

In vivo Galleria mellonella survival assay

Waxworms were purchased from an online bait shop (www.rainbowmealworms.org) and stored at room temperature until injection. Waxworms weighing 180-230 mg were selected into groups of 10 for injection. Overnight cultures of WT, 4D5, 11F11, LV1, and LV2 were grown using a 1 colony in 3 mL of BHI. The day of injection, 100 µl of overnight culture was added to 3 mL of BHI to create day cultures that were grown up to an optical density of approximately 0.4 (log phase). Upon reaching log phase, the bacterial cultures were washed and resuspended in 3 mL of phosphate buffered saline (PBS). A 1:2 dilution was created by adding 500 µl of the bacterial culture to a microcentrifuge tube containing 500 µl of PBS. Each waxworm was injected in the posterior cuticle with 10 µl of this 1:2 dilution using a 27-gauge needle and automated pump. After injection, the waxworms were incubated at 37°C, and their survival was monitored over the course of 72 hours and recorded in 24-hour increments. To ensure that equivalent amounts of bacteria was injected into the waxworms between experimental groups, 10-fold serial dilutions of the 1:2 diluted cultures was plated on BHI plates and incubated at 37°C. Approximately 16 hours after incubation, colonies were counted, and colony-forming units (CFU) were calculated. If there was greater than a 10-fold difference in CFU's between experimental groups, results were discarded. Additionally, controls were conducted to ensure the subset of worms used were healthy and that the injection technique used was consistent with previous assays. If more than 30% of worms injected with PBS died, results were discarded.

In vivo Galleria mellonella competition assay

Waxworms were purchased from an online bait shop (www.rainbowmealworms.com) and stored at room temperature until injection. Waxworms weighing 180-230 mg separated into

subsets of 5 worms and injected with a mixture of two bacterial strains. Overnight cultures of WT, 4D5, 11F11, LV1, and LV2 were grown using a 1 colony in 3 mL of BHI. The day of injection, 100 µl of overnight culture was added to 3 mL of BHI to create day cultures that were grown up to an optical density of approximately 0.4 (log phase). Upon reaching log phase, a 1:1 mixture was created by combining 500 µl of WT bacteria with 500 µl of LV1, LV2, and 11F11, respectively. Each waxworm was then injected in the posterior cuticle with 10 µl of this 1:1 mixture using a 27-gauge needle and automated pump. After injection, the waxworms were incubated at 37°C for 6 hours before being rinsed in 100% pure EtOH for approximately 10 seconds and subsequently miliQ water for 5 seconds. Then, the rinsed worm was placed in an impact-resistant screw cap tube with 400 µl PBS and approximately 250 µl of 1 mm ceramic beads. Two bead beating cycles were then conducted for 45 seconds at 4.5 meters per second to homogenize the worm. The homogenized mixtures were then diluted down to 1:100,000 dilution in a 96-well plate and the 1:1000, 1:10,000, 1:100,000, and 1:100,000 dilutions were plated on both BHI and BHI kanamycin plates. These plated dilutions were incubated for approximately 20 hours at 30 °C before WT and transposon mutant bacterial colony recovery rates were determined by counting colonies and subsequently calculating colony-forming units (CFU). Additionally, three controls were used to ensure we had a true 1:1 mixture before and after injecting into the waxworms. Upon reaching log phase and creating the 1:1 mixture, the mixture was plated on BHI and BHI kanamycin plates. After injection into the waxworms, a few waxworms were homogenized, and a 0-hour post infection bacterial solution was plated on BHI and BHI kanamycin plates. Additionally, the 1:1 mixture was homogenized before injection into the waxworms, and this homogenized mixture was plated on BHI and BHI kanamycin plates.

Confirmation of transposon insertion site

The site of transposon insertion was found using a Y-linker protocol developed previously [16]. Reference Table 1 for a complete list of primers used in this protocol. 18 µl of *NlaIII* Linker 2 stock (100 µM) was added to a microcentrifuge tube with 2 µl of PNK (T4 Polynucleotide ligase) (NEB M0201S), 4 µl 10x T4 ligase buffer, and 16 µl H_2O. *NlaIII* Linker 2 was then phosphorylated by incubating this microcentrifuge tube at 37 °C for one hour. After one hour, PNK is heat denatured at 65 °C for 20 minutes. Then, 18 µl of *NlaIII* Linker 1 stock (100 µM) was added to this mixture to a final volume of 58 µl. The mixture is then heated to 95 °C in a heat block for 5 minutes. After five minutes, the heat block was turned off, and the tubes were left inside the heat block for a minimum of 4 hours. This process yielded the Y-linker. Next, 5 µg of genomic DNA from LV1, LV2, or 11F11 was digested with 5 µl *NlaIII* (NEB) for 2 hours at 37 °C. Then, approximately 200 ng of digested DNA was ligated to 5 µl Y-linker with 1 µl T4 DNA ligase and 2 µl of 10x T4 ligase buffer for a total volume of 20 µl. This mixture was incubated overnight at room temperature. The following day, this ligation was diluted by adding 180 µl H_2O to the microcentrifuge tube. To denature T4 DNA ligase, the tube was heated at 65 °C for 10 minutes. This was used as the template DNA in PCR with the Y-linker primer and Himar 1-2 long primer. After a successful PCR was verified with a strong band using gel electrophoresis, the product was sequenced using Himar 1-4 and the results were BLASTed against the *B. anthracis* genome. After BLAST analysis, we confirmed the site of transposon insertion by using colony PCR where one colony was mixed with 10 µl of H_2O in a PCR tube and microwaved for 1 minute. 1 µl was taken from this microwaved mixture and used as genomic DNA in the confirmation PCR along with Himar 1-2 Long and 11F11 Confirm Rev primer or LV1 Confirm Rev primer.

Table 1. Primers used in Y-linker PCR and Confirmation PCR

Primer Name	Primer Sequence
Y-linker (3-60)	5’ – CTGCTCGAATTCAAGCTTCT – 3’
NlaIII Linker 1 (3-61)	5’ – TTTCTGCTCGAATTCAAGCTTCTAACGATGTACGGGGACACATG – 3’
NlaIII Linker 2 (3-62)	5’ – TGTCCCCGTACATCGTTAGAACTACTCGTACCATCCACAT – 3’
LV1 Confirm Rev (9-14)	5’ – GTATTGTCGTTTCCCTTCTTCACG – 3’
11F11 Confirm Rev (9-21)	5’ – CAGTTGCACTTGGAGAGAACG – 3’
Himar 1-2 Long (3-58)	5’ – GGGAATCATTTGAAGGTTGGTACT – 3’
Himar 1-4 (3-1)	5’ – TATGCATTTAATACTAGCGAC – 3’

Creation of insertional mutant

The LV1 insert, a region of homology to the interrupted gene in LV1, was cloned into pHY304, a targeting vector. To amplify this region of homology, I performed a polymerase chain reaction (PCR). I took one colony of wild-type *B. anthracis* Sterne, mixed it with 10 µl of sterile H_2O, and microwaved it for 1 minute. To create the PCR mixture, I added 5 µl of 10x PCR buffer, 5 µl deoxynucleotide triphosphates (dNTPs), 2.5 µl Taq, 2.5 µl of LV1 IM Fwd

XhoI primer (Table 2), 2.5 µl of LV1 IM Rev SalI-HF primer (Table 2), and 30 µl H_2O. This mixture was amplified using PCR, and gel electrophoresis at 90 V for 35 minutes was performed to confirm amplification. 10 µl of loading dye and gel green was added into each PCR tube, and 5 µl of each PCR product was added to separate wells on the 1 % agarose gel to be compared against 5 µl of Ladder A in well 1. The final concentration of this LV1 insert was determined to be 82.0 ng/µl using a nanodrop spectrophotometer. Next, a digestion was performed of the LV1 insert and pHY304 plasmid vector, respectively. 41 µl of the LV1 insert (82.0 ng/µl), 5 µl rcutsmart buffer, 2 µl of XhoI restriction enzyme, and 2 µl of SalI-HF restriction enzyme was added to a 1.5 ml microcentrifuge tube. In a separate microcentrifuge tube, 6.5 µl of purified pHY304 (844 ng/µl), 5 µl rcutsmart buffer, 2 µl of XhoI restriction enzyme, 2 µl of SalI-HF restriction enzyme, and 34.5 µl of sterile H_2O was added. Both microcentrifuge tubes were then incubated at 37 °C for 4 hours. For the final 30 minutes of incubation, 2 µl of calf-intestinal alkaline phosphatase (CIP) was added to dephosphorylate the terminal ends of the targeting vector. After the digestion was completed, the digested LV1 insert and targeting vector were purified using the Promega Wizard SV Gel and PCR Clean-Up System. Using the nanodrop, the concentrations of the LV1 insert and plasmid were determined to be 14.0 ng/µl and 12.7 ng µl, respectively. Next, I ligated the digested LV1 insert to the pHY304 plasmid by adding a 5:1 molar ratio of insert to plasmid, while still ensuring I was ligating at least 50 ng of the pHY304 plasmid. I added 2.0 µl of digested LV1 insert, 4 µl of digested pHY304, 2 µl of 10x ligation buffer, 1 µl of NEB DNA ligase, and 11 µl of sterile H_2O to create a 20 µl total volume for this reaction. I also performed a control ligation without the digested LV1 insert and only 4 µl of digested pHY304, 2 µl of 10x ligation buffer, 1 µl of NEG DNA ligase, and 13 µl of sterile H_2O.

Both reactions incubated at room temperature overnight to create the ligated plasmid for subsequent transformation into *Escherichia Coli* and *B. anthracis.*

For the first transformation into *E. coli,* I thawed out 50 µl of commercial electrocompetent Lucigen *E. coli* MC1061 in an ice bath. Once the *E. coli* cells were thawed, I added 1 µl of the ligation from above and let the mixture sit in the ice bath for 10 additional minutes. Then, this 51 µl mixture was transferred to an electroporation cuvette and shocked at a voltage of 1800 mV in the electroporator. Immediately after shocking the cells, 950 µl of SOC recovery media was added to the cuvette. Then, this mixture was transferred to a 1.5 ml microcentrifuge tube and incubated at 30 °C for 1.5 hours. Following this incubation, 4 separate dilutions were plated from each microcentrifuge tube on Erm500 antibiotic plates and incubated at 30 °C in static conditions for 2-3 days. Growth was monitored, and any colonies that grew were subject to colony PCR using the pHY3065Fwd (Table 2) and pHY3260Rev (Table 2) primers followed by gel electrophoresis to confirm amplification of a region of the plasmid.

After a band was observed on the gel, overnight cultures were made using 1 colony of the transformed MC1061 cells and 3 mL of BHI Erm500 broth. The plasmid was then purified out of the MC1061 cells using the IBI Scientific High-Speed Plasmid Mini Kit. Then, a second electrocompetent transformation was conducted using *E. Coli* GM2163 cells, which are methylation deficient. The protocol used for the *E. coli* MC1061 transformation was repeated, and the presence of the plasmid was verified using colony PCR and the pHY3065Fwd (Table 2) and pHY3260Rev (Table 2) primers. Gel electrophoresis was conducted to confirm the amplification of a region of the plasmid. The plasmid was then purified out of the GM2163 cells using the IBI Scientific High-Speed Plasmid Mini Kit, and a 244.1 ng/µl concentration was determined using the nanodrop.

Next, the final electrocompetent transformation into *B. anthracis* was conducted. To make *B.* anthracis competent, overnight cultures were started at 37°C in shaking conditions using 1 colony of wild-type *B. anthracis* and 3 mL of 0.5 % glycerol BHI. The following day, 0.5 mL of the ON culture was transferred to a sterile 500 mL Erlenmeyer flask with 60 mL 0.5% glycerol BHI and incubated at 37 °C in shaking conditions. Once an optical density of 0.6-0.8 was reached, the *B. anthracis* cells were collected using a 500 mL, 0.22 µm, PES 90mm membrane diameter bottle top filter apparatus and applying vacuum**.** Cells were then washed with 25 mL of ice-cold electroporation buffer (1mM HEPES 10% glycerol pH 7.0) by pipetting the culture on top of the filter up and down several times before applying vacuum to get rid of the buffer. This wash was repeated two additional times. Cells were then suspended in $1/20^{th}$ the original volume (3 mL) of electroporation buffer, added to a 5 mL culture tube, and placed in an ice bath for 15 minutes. 2.5 µl of the purified plasmid (244.1 ng/µl) from the step above was added to a 0.1 cm gap electroporation cuvette with 80 µl of the washed *B. anthracis* cells and kept on ice for 15 minutes. Next, the *B. anthracis*-plasmid mixture was shocked at a voltage of 1800 mV in the electroporator. Immediately after shocking the cells, 500 µl of BGGM recovery media (BHI containing 10% glycerol, 0.4% glucose, and 10 mM $MgCl_2$) was added to the cuvette. The contents of the cuvette were then transferred to a 1.5 mL microcentrifuge tube and incubated at 30°C shaking conditions for 1.5 hours. For each transformation conducted, 100 µl was plated two times on two Erm5 plates and 150 µl was plated two times on two Erm5 plates. These plates were then incubated at 30 °C static conditions for 2 days. Growth was monitored, and any colonies that grew were subject to colony PCR using the pHY3065Fwd (Table 2) and pHY3260Rev (Table 2) primers followed by gel electrophoresis to confirm amplification of a region of the plasmid.

Next, the insertional mutant was constructed. Overnight cultures of 1 colony of electrocompetent *B. anthracis* were grown with 3 mL Erm5 BHI at 30 °C shaking conditions. The following day, 100 µl of overnight culture was added to 5 mLs BHI Erm5 BHI and grown at 37 °C shaking conditions for 8 hours. Then, the culture is diluted down to 1:500, 1:1000, 1:5000, and 1:10,000 in 1.5 mL microcentrifuge tubes. 100 µl of each dilution was plated on Erm5 plates and incubated overnight at 37 °C static conditions. Once colonies appeared the following day, 7 colonies were picked and subject to colony PCR using pHY3065Fwd (Table 2) and LV1 Confirm Rev (Table 1) to verify the LV1 insert has integrated into the *B. anthracis* genome.

Table 2. Primers used in Creation of Insertional Mutant

Primer Name	Primer Sequence
LV1 IM Fwd XhoI (9-19)	5’ – ACAGTCTCGAGCACAACGTCCTACCCTGGTT – 3’
LV1 IM Rev SalI-HF (9-20)	5’ – TACCGTCGACCGCAGCTACTACTCTATCTTGCTC – 3’
pHY3065Fwd (3-34)	5’ – ACGACTCACTATAGGGCGAATTGG – 3’
pHY3260Rev (7-5)	5’ – GCGGATAACAATTTCACACAGG – 3’

RESULTS

In vitro screen in 96-well plates identifies 2 novel transposon mutants.

We began this screen with the goal of screening around 1,000 mutants from the transposon mutant library for increased susceptibility to hydrogen peroxide compared to WT. Initially, we determined the appropriate concentration of H_2O_2 where we observed attenuated growth for our positive controls, 4D5 and 11F11, but not WT bacteria. We tested the concentrations 0%, 0.02%, 0.03%, 0.035%, 0.04%, 0.05%, 0.06%, 0,07%, 0.08%, 0.1%, 0.12%, 0.14%, 0.16%, and 0.2% H_2O_2-BHI and determined 0.035% H_2O_2-BHI to be the concentration where we observed consistent attenuation of growth of 4D5 and 11F11 but no attenuated growth of WT. Once we identified the optimal H_2O_2 concentration, we performed the procedure seen in Figure 1. Bacteria were initially plated on kanamycin plates from the transposon mutant library. Colonies were placed into individual wells in a 96-well plate with BHI to be grown overnight before being challenged with 0.035% H_2O_2-BHI in a new 96-well plate. Wells with no growth were further screened to confirm the observed phenotype. We identified 34 mutants that showed attenuated growth in our first pass of the 1,000 mutants before going back to perform 8 independent MIC assays of our initial hits to test for consistent attenuation of growth. In these 8 assays, we increased our H_2O_2-BHI solution to 0.1%, which is where we saw the most distinguishable phenotype between our mutants and WT. Two mutants had statistically significant attenuation of growth in the 8 independent assays conducted in the primary screen, and we named them LV1 and LV2. The growth comparison of LV1 and LV2 to WT, 4D5, and 11F11 is depicted in Figure 2.

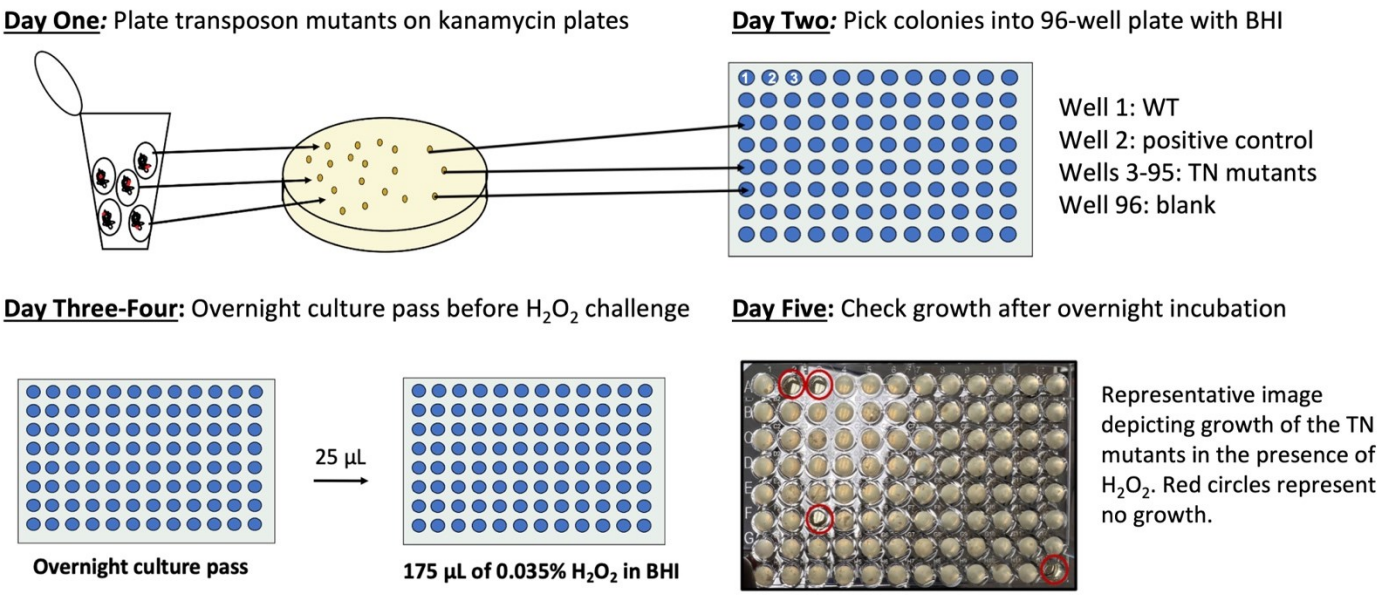

Figure 1. Schematic of *in vitro* H_2O_2 assay screen. Schematic outlining the five-day screening protocol.

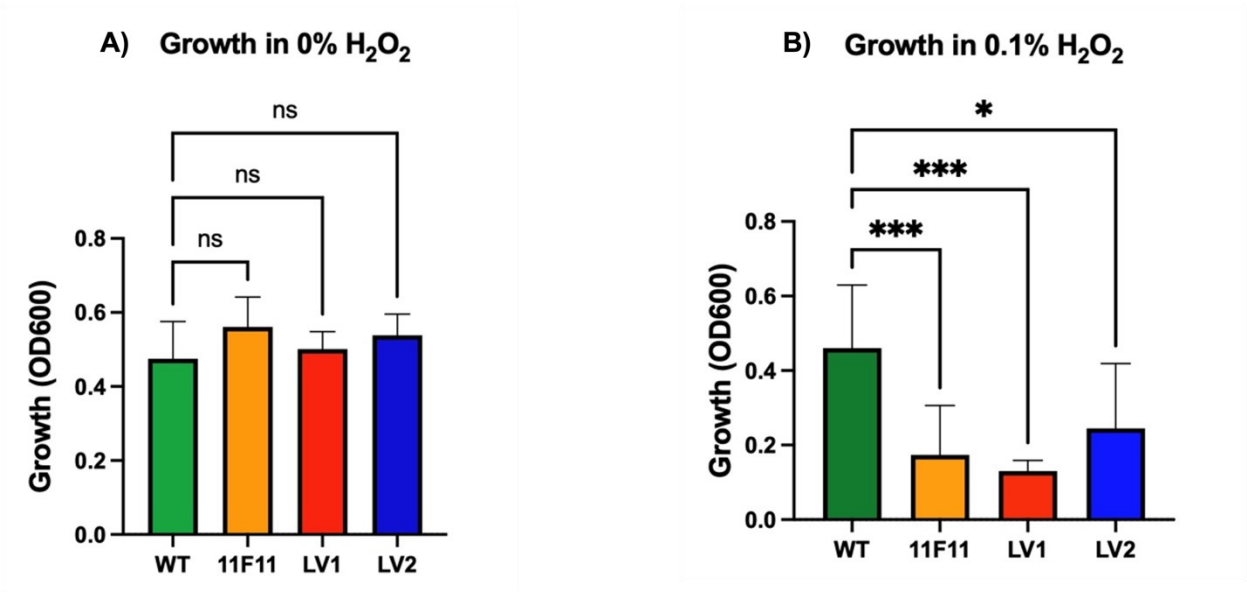

Figure 2. Two transposon mutants exhibit H_2O_2 susceptibility from 96-well plate screen. Growth of WT, 11F11, LV1, and LV2 in A) 0% and B) 0.1% H_2O_2 in BHI media at stationary phase conditions. The 96-well plates were screened 8 independent times and is presented as the mean +/- standard deviation. In the panels above, statistical significance between WT and mutant is designated with *p<0.05, **p<0.01, ***p<0.001, and ****p<0.0001 one-way ANOVA followed by Dunnett's multiple comparison post-hoc test.

To confirm this observed phenotype, I performed a secondary screen growing LV1 and LV2 overnight in larger volume 16 mL culture tubes versus the 96-well plate, which should promote better aeration and overall growth of the bacteria. For this secondary screen, I began using a newer hydrogen peroxide solution than the one used in the primary screen, so I performed a gradient screen of varying H_2O_2-BHI concentrations to see where the growth of my positive controls, 4D5 and 11F11, would be attenuated but not WT bacteria. This screen was performed in a 96-well plate with the concentrations 0%, 0.002%, 0.003%, 0.004%, 0.005%, 0.006%, 0.008%, and 0.01% H_2O_2-BHI. I determined 0.004% H_2O_2-BHI to be the concentration in this secondary screen at stationary phase where we observed consistent attenuation of growth of 4D5 and 11F11 but not WT. After performing 5 independent MIC assays with the mutants, I observed that LV2 no longer demonstrated increased susceptibility to H_2O_2 while LV1 had a slightly weaker phenotype than previously observed, which can be seen in Figure 3. Due to this change in the phenotype, I was curious to see if the phenotype remained with bacteria in their highly replicative phase, logarithmic phase, which is also the phase of bacteria we use in *in vivo* assays. I repeated the gradient screen using the same concentrations from stationary phase, and I determined 0.005% H_2O_2-BHI to be the concentration in this secondary screen at logarithmic phase where we observed consistent attenuation of growth of 4D5 and 11F11 but not WT. Interestingly, all mutants lost their phenotype, and we observed no statistically significant attenuation of growth compared to that of WT.

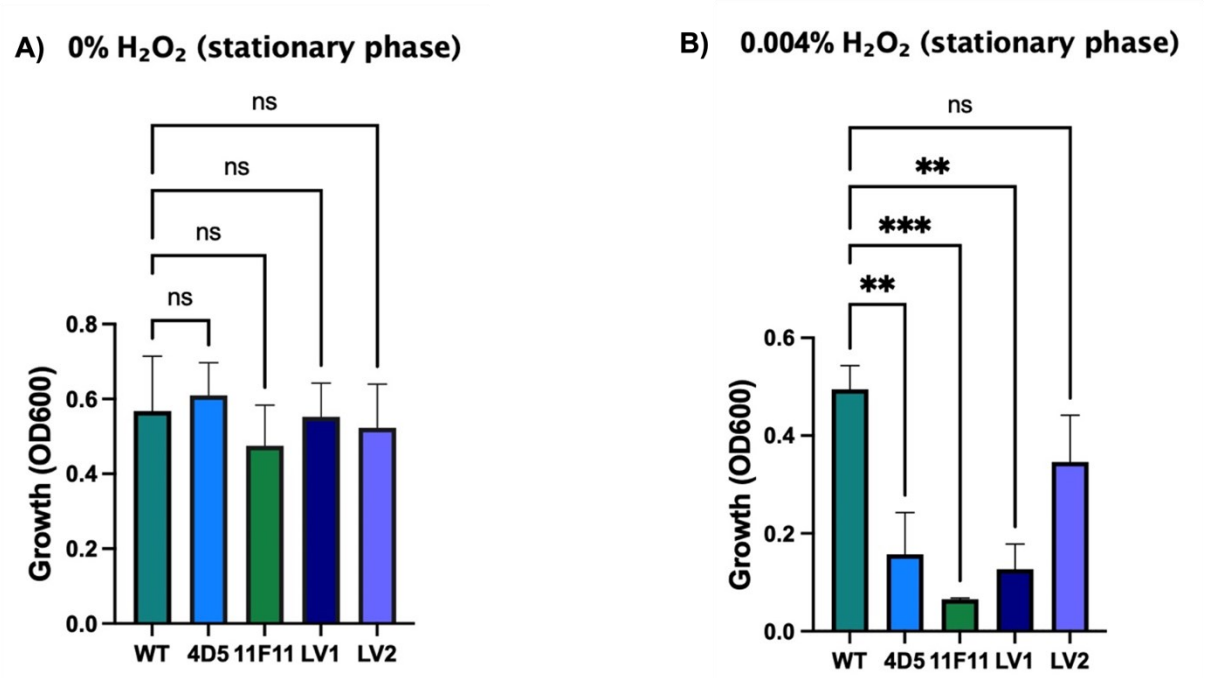

Figure 3. LV1 but not LV2 retains phenotype using large-volume cultures. Growth of WT, 4D5, 11F11, LV1, and LV2 in A) 0% and B) 0.004% H_2O_2 in BHI media. The 96-well plates were screened 5 times with error bars indicating standard deviation. In the panels above, statistical significance between WT and mutant is designated with *p<0.05, **p<0.01, ***p<0.001, and ****p<0.0001 one-way ANOVA followed by Dunnett's multiple comparison post-hoc test.

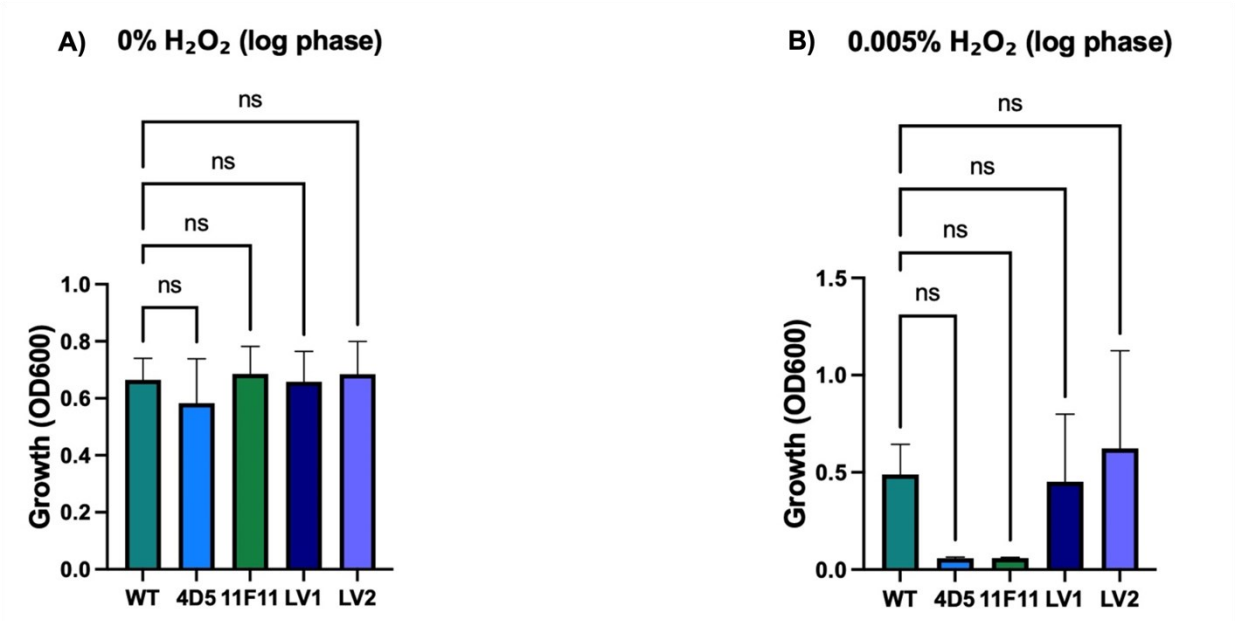

Figure 4. Large volume logarithmic phase cultures show no H_2O_2 susceptibility. Growth of WT, 4D5, 11F11, LV1, and LV2 in A) 0% and B) 0.004% H_2O_2 in BHI using cultures grown to log phase. The 96-well plates were screened 4 times with error bars indicating standard deviation. In the panels above, statistical significance between WT and mutant is designated with *p<0.05, **p<0.01, ***p<0.001, and ****p<0.0001 one-way ANOVA followed by Dunnett's multiple comparison post-hoc test.

Comparable growth observed between TN mutants and WT.

To evaluate the contribution of the interrupted gene in LV1, LV2, 11F11, and 4D5 in *B. anthracis Sterne* growth, I monitored growth of all mutants compared to wild-type *B. anthracis* at 37 °C for 6 hours. The results seen in Figure 5 suggest that the interrupted genes in 11F11, LV1, and LV2 do not drastically affect growth rates in comparison to wild-type *B. anthracis* but 4D5, a previously characterized transposon mutant [15] that we have used as a positive control, shows evidence of decreased growth rate relative to wild-type.

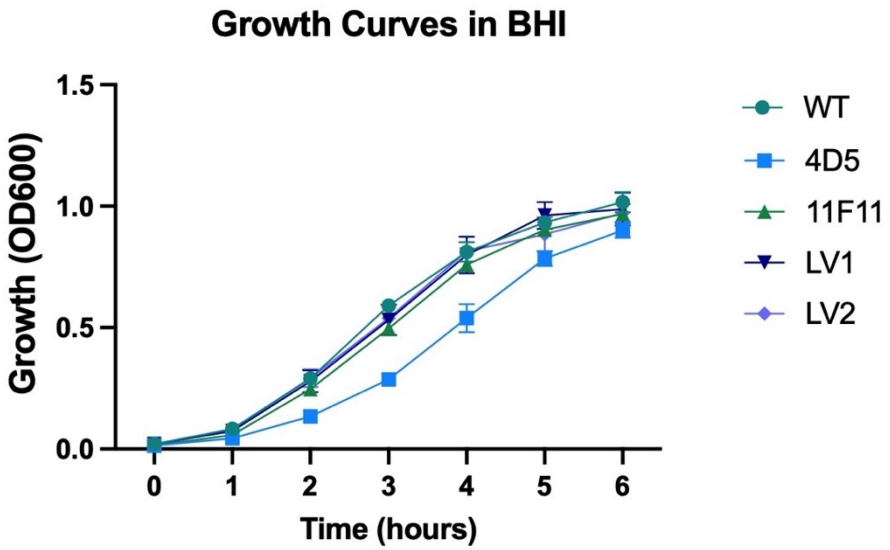

Figure 5. LV1 and LV2 show normal growth patterns in BHI. The growth of WT, 4D5, 11F11, LV1, and LV2 was monitored over the course of 6 hours at 37° C. This experiment was performed 3 independent times and is presented as the mean with error bars indicating standard deviation.

Survival assay in G. mellonella identifies reduced virulence in LV1.

The novel mutants LV1 and LV2 were identified as mutants of interest from our primary screen. To test their virulence, we used the *G. mellonella in vivo* model, which has a very distinguishable phenotype when the worms are alive or dead. When the worms are alive, they are a cream-white color and turn black when they die, as seen in Figure 6C. Worms weighing

between 180 mg and 230 mg were used for infection. The average worm masses were all approximately the same for each bacterial strain, and this can be observed in Figure 6A. This is important because we want to ensure the ratio of bacteria injected to mass of the worm was approximately equivalent. In this assay, wild-type bacteria, our positive controls, and LV1 and LV2 were grown up to logarithmic phase (optical density= 0.4-0.5) before being washed and diluted 1:2 in PBS. Then, 10 µl of this diluted culture was injected into the corresponding subset of worms (10 worms per bacterial strain). A schematic of this procedure can be seen in Figure 6B. To ensure we were injecting an equivalent number of bacteria into different subsets of worms, we plated and calculated the colony forming units per mL for each bacterial strain, and they were all found to be approximately equivalent.

After injection, worm survival was monitored over the course of 72 hours in 24-hour increments. Percent waxworm survival can be observed in Figure 7 for injection with 4D5, LV1, LV2, and 11F11 compared to PBS and WT. The subset of worms injected with PBS served as our negative control to ensure the process of injecting fluid into the worms was not lethal. This proved to be the case with high survival rates of approximately 85%. Worms injected with wild-type bacteria demonstrated relatively lower survival rates of 20% and 35%, respectively. 4D5 served as our positive control, which has previously been shown to have attenuated virulence, and this subset had a relatively higher survival rate of nearly 50%. This survival rate of worms injected with 4D5 is slightly lower than observed in previous studies but still statistically significant compared to WT in these assays [15, 17]. LV2 is seen to have a relatively higher survival rate like 4D5 at approximately 55%, which is a statistically significant higher survival rate than wild-type. LV1 and 11F11 exhibit comparable survival rates as wild-type at 20%. Therefore, these results suggest that LV2 is attenuated in an invertebrate model *in vivo.*

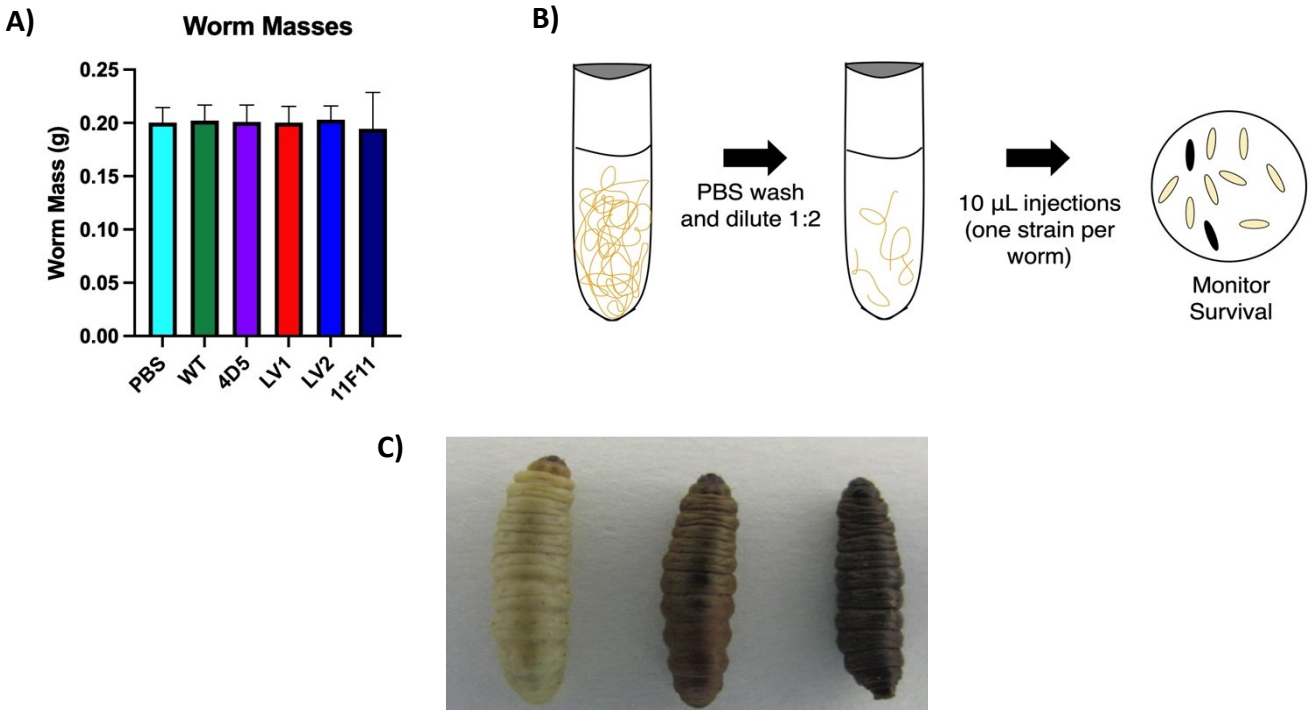

Figure 6. ***In vivo G. mellonella*** **infection assay. A)** Worm masses for each injection group were recorded, and the average weight is shown with error bars indicating standard deviation. **B)** Schematic of the general protocol for this infection assay. **C)** Comparison of the range of phenotypes seen with this worm model. A living infected worm is pictured on the left, a dying infected worm is pictured in the middle, and a dead infected worm is pictured on the right.

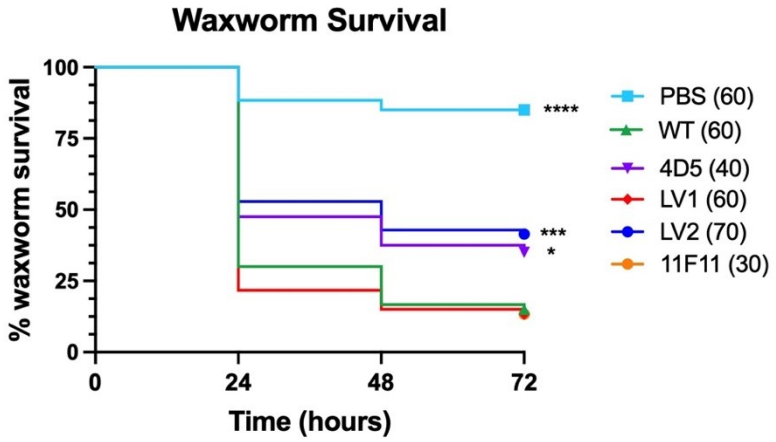

Figure 7. Mutants 4D5 and LV2 show attenuated virulence in ***G. mellonella.*** Percent survival of worms injected with PBS (saline), wild-type *B. anthracis* (WT), and the transposon mutants 4D5, LV1, LV2, and 11F11 at 24 ,48, and 72 hours. This assay was performed 6 independent times, and the total number of worms in each injection group are indicated in parenthesis. Significant difference in survival compared to WT is indicated by *p<0.05, ***p<0.001, and ****p<0.0001 using log-rank statistical analysis.

Competition assay in G. mellonella identifies reduced virulence in 11F11, LV1, and LV2.

Another way to assess the virulence of our bacterial strains is through a competition assay where one worm is infected with both WT and mutant *B. anthracis.* This puts both bacterial strains in direct competition with each other, and the more virulent strain will proliferate more and have a higher percent bacterial recovery rate.

To put these bacterial strains in direct competition with each other, I grew day cultures up to log phase of WT, 11F11, LV1, and LV2. Once an optical density of 0.4 was achieved, I combined WT and mutant at a 50:50 ratio before injecting the mixture into a subset of 5 waxworms. Then I incubated the worms at 37° C for 6 hours before homogenizing, washing, and plating the mixture onto BHI and BHI-Kan 50 plates. WT colonies can only grow on non-antibiotic media, whereas the transposon mutant colonies can grow on both antibiotic and non-antibiotic media. To determine WT percent recovery, we took the number of WT colonies, divided that number by the total number of colonies on BHI before multiplying by 100. A schematic of this procedure can be seen in Figure 8.

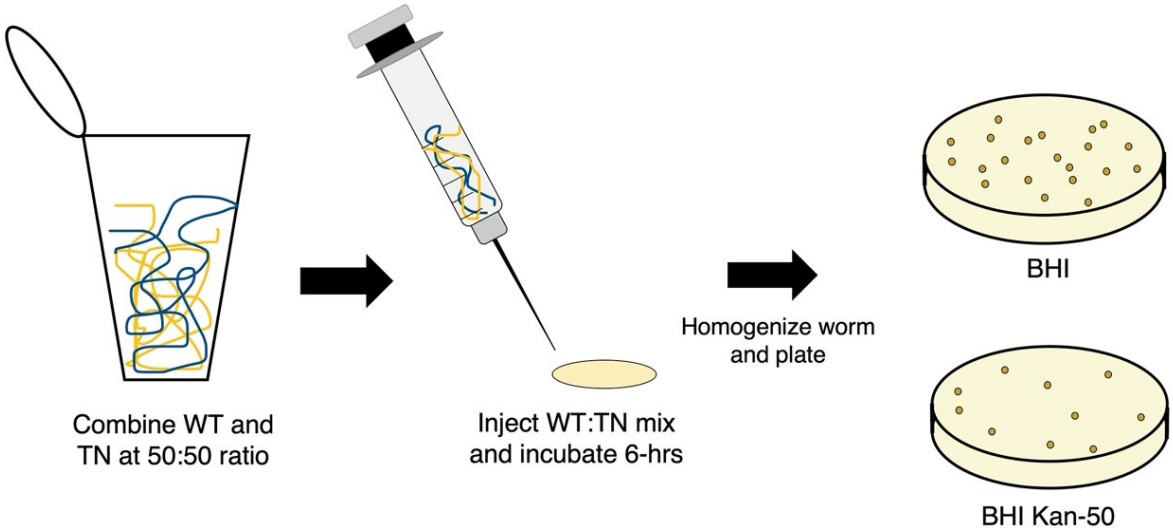

Figure 8. *G. mellonella* competition assay. Overnight cultures of wild-type (WT) and the transposon (TN) mutants 11F11, LV1, and LV2 are grown up to log phase before being combined at a 50:50 ratio. The WT:TN mixture is washed with PBS before being injected into the worms. After incubation for 6 hours, worms are homogenized and plated on BHI and BHI-kanamycin plates to compare WT versus mutant colony forming units.

To validate this assay, we performed three controls to ensure we were truly injecting a 50:50 mixture into the worms. The first of these was simply plating the 50:50 mixture on BHI and BHI Kan-50 plates, and, as expected we saw a 50:50 ratio of WT:mutant colonies (Figure 9A, Figure 10A, Figure 11A). Next, we performed a lysis control to ensure the action of bead beating did not lyse mutant and wild-type bacteria and different rates, and we did not observe any statistically significant difference in the lysing rates (Figure 9B, Figure 10B, Figure 11B). Lastly, we injected a subset of worms and homogenized and plated the mixture immediately after injection to yield a 0-hour post infection time point. We still observed no statistically significant difference in percent bacterial recovery rates (Figure 9C, Figure 10C, Figure 11C).

After the infected larvae were incubated at 37° C for six hours, the worms were placed in impact-resistant screw cap tubes with 400 µl PBS and homogenized, washed, and plated on BHI and BHI Kan-50 plates. After counting colonies the following morning, we observed statistically significant decreases in the percent bacterial recovery rates for 11F11, LV1, and LV2 compared to WT percent bacterial recovery rates (Figure 9D, Figure 10D, Figure 11D). This shows us that all three mutants are attenuated, and the transposon interrupting a gene in the bacterial genome may be contributing to their reduced virulence.

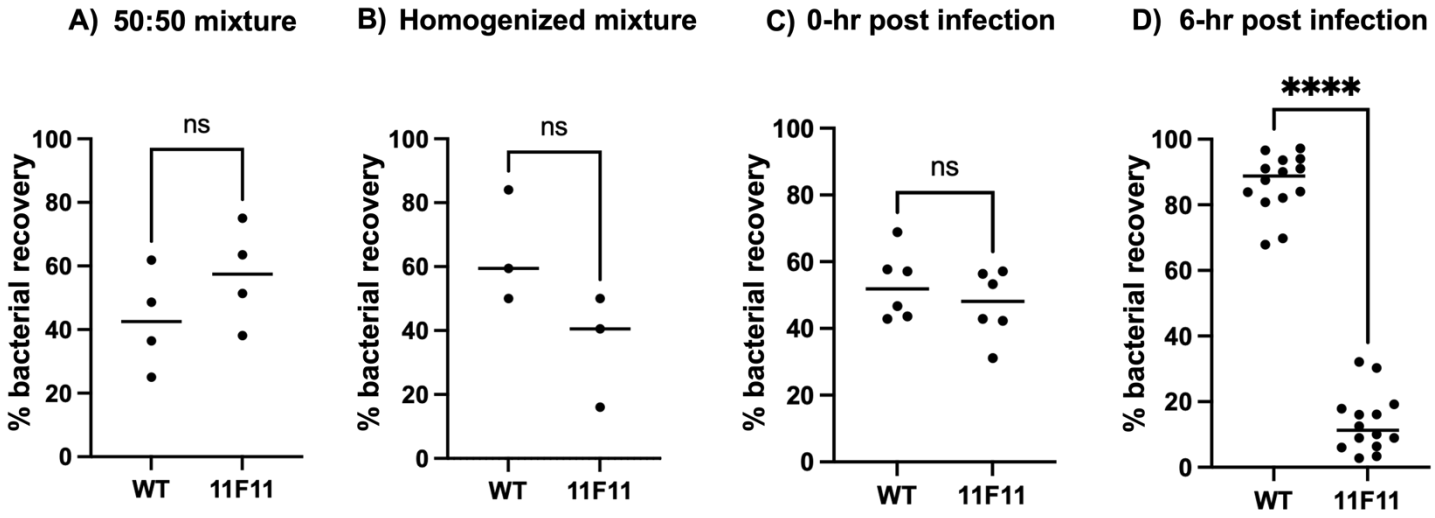

Figure 9. 11F11 demonstrates decreased virulence *in vivo* in competition with wildtype. A) Recovery of 11F11 and wild-type after mixing at a 1:1 ratio. **B)** Recovery of 11F11 and wild-type after mixing at a 1:1 ratio and then homogenizing. **C)** Percent of WT or 11F11 recovered immediately following injection into worms. **D)** Percent of WT or 11F11 recovered 6 hours after injection into worms. Statistical significance between WT and 11F11 is indicated by *p<0.05, ***p<0.001, and ****p<0.0001 using paired t-test statistical analysis.

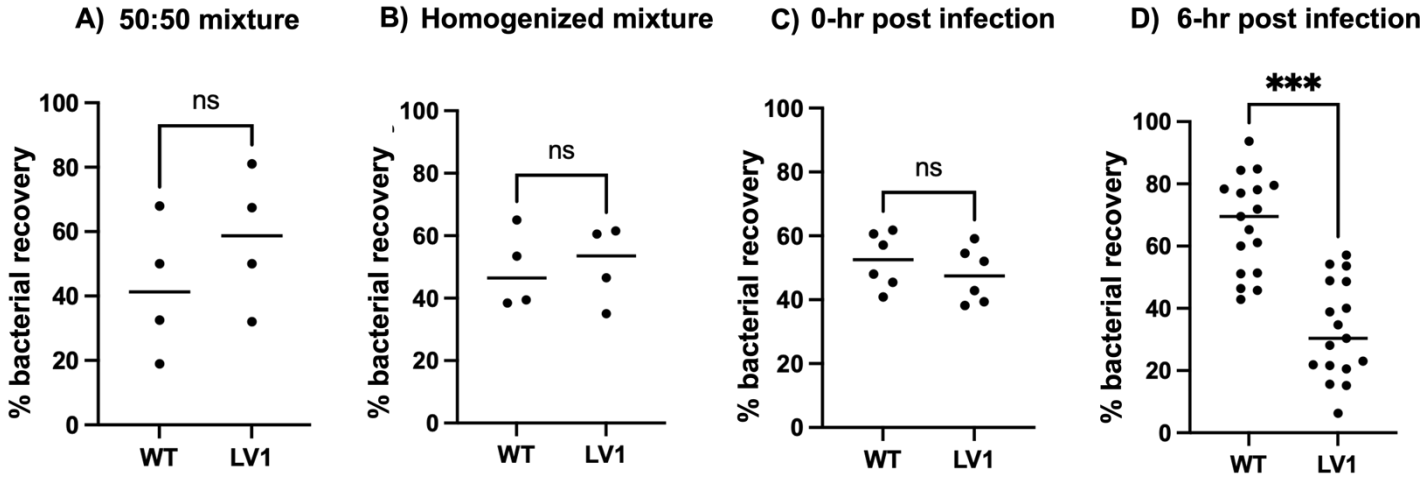

Figure 10. LV1 demonstrates decreased virulence *in vivo* in competition with wildtype. A) Recovery of LV1 and wild-type after mixing at a 1:1 ratio. **B)** Recovery of LV1 and wild-type after mixing at a 1:1 ratio and then homogenizing. **C)** Percent of WT or LV1 recovered immediately following injection into worms. **D)** Percent of WT or LV1 recovered 6 hours after injection into worms. Each dot represents a separate room and experiment was repeated 2 independent times. Statistical significance between WT and LV1 is indicated by *p<0.05, ***p<0.001, and ****p<0.0001 using paired t-test statistical analysis.

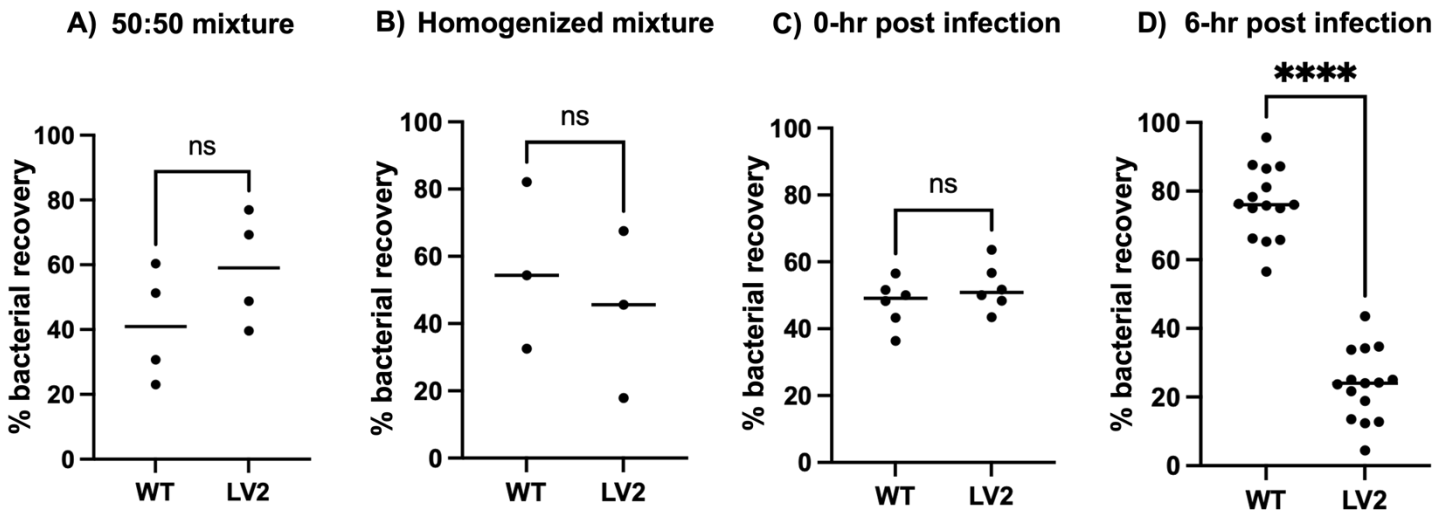

Figure 11. LV2 demonstrates decreased virulence *in vivo* in competition with wildtype. A) Recovery of LV2 and wild-type after mixing at a 1:1 ratio. **B)** Recovery of LV2 and wild-type after mixing at a 1:1 ratio and then homogenizing. **C)** Percent of WT or LV2 recovered immediately following injection into worms. **D)** Percent of WT or LV2 recovered 6 hours after injection into worms. Statistical significance between WT and LV2 is indicated by *p<0.05, ***p<0.001, and ****p<0.0001 using paired t-test statistical analysis.

Successful identification of the insertion site in LV1 and 11F11.

Following *in vitro* and *in vivo* testing of these mutants, the next step was to determine the insertion site of our transposon. At this point, I was still unsure of what gene(s) are being interrupted by our transposon, so I performed Y-linker PCR [16]. With this method, the digested DNA (Figure 12, gray sequence), which was previously extracted via a genomic DNA prep, is ligated to a Y-linker (Figure 12, purple sequence). This Y-linker ligates because it has *NlaIII* compatible sticky ends, and *NlaIII* was the restriction enzyme used in the digest. PCR was then conducted using a transposon specific primer (Figure 12, red arrow) and a Y-linker specific primer (Figure 12, purple arrow). This amplified the specific region of DNA where there was a section of transposon sequence flanking a section of the bacterial chromosome.

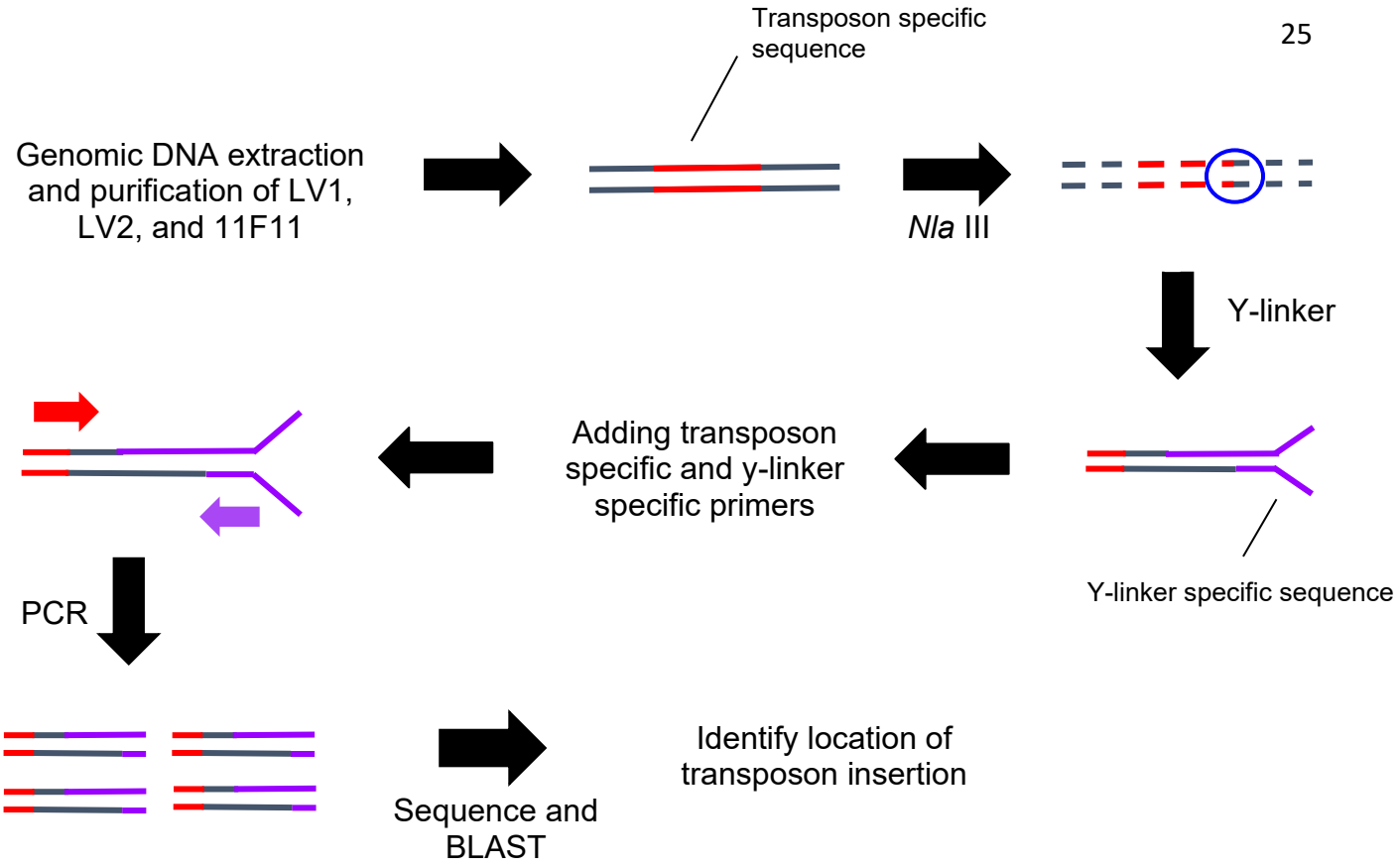

Figure 12. Identification of transposon insertion. The genomic DNA (gray) containing a transposon insertion (red) is digested with *NlaIII*, a restriction enzyme. The Y-linker (purple) anneals to digested genomic DNA. PCR is conducted using a transposon specific primer (red) and y-linker specific primer (purple) to amplify the transposon-disrupted gene.

Successful amplification was verified with gel electrophoresis, and a band was observed at approximately 400 bp for both LV1 (Figure 13) and 11F11 (not pictured). After amplification, we sequenced and analyzed via BLAST to determine the insertion site. This protocol was successfully performed with LV1 and 11F11, and their BLAST sequences can be observed in Figure 14 and Figure 15, respectively. I confirmed both insertion sites via a colony PCR using the same transposon specific primer (Figure 16, FWD black arrows) and a primer downstream of the disrupted gene (Figure 16, REV black arrows). A band was observed at approximately 400 bp for both mutants, confirming their respective gene disruptions. The transposon inserted in LV1 is inserted in a gene encoding a collagenase-like protein while the transposon inserted in 11F11 is inserted in a gene encoding a catalase enzyme (Figure 16).

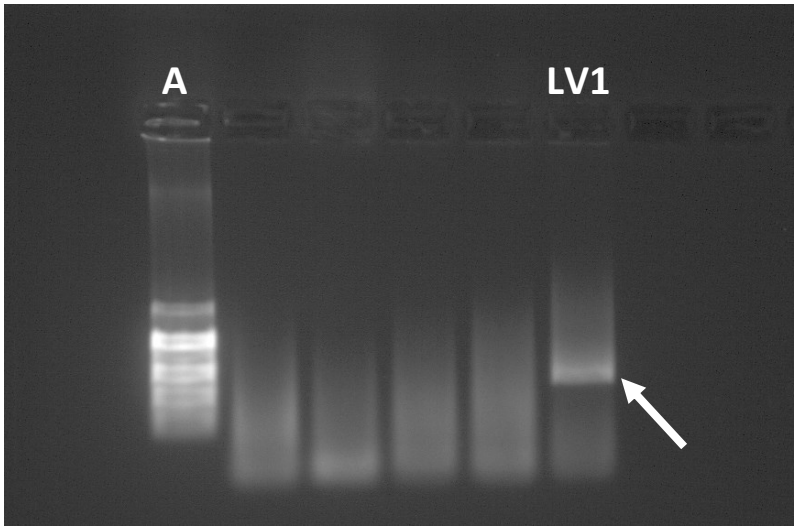

Figure 13. Gel electrophoresis of LV1 Y-linker PCR product. PCR amplification of digested LV1 genomic DNA after ligation to a Y-linker. PCR was successful was using the Y-linker primer and Himar 1-2 long primer. Mutant LV1 is indicated by the arrow.

```
  1 CCTGACCGACGGGGCATATCAGCCAACCTGTTACGTATGTAAGCGATTATGCGAAAGGACAAGCTGTATATGAAATTGTAAAAGGAATTGATTATGATAT
101 ACAGTCTTATTTGCAAGATACGAATAAGCAACCTAATGAAACAATGTGGTATGGAAAGATTGATAACTTTATAAATGAGGTTAATAGAATTGCTCTCGTG
201 GGGAATATAACAAATGAAAATAGTTGGCTAATTAATAATGGCATTTATTATGCAGGTCGTTTAGGGAAATTTCATAGTAATCCATACAAAGGATTGGAAG
301 TTATTACACAAGCAATGAGCTTGTATCCTCGTCTAAGTGGACCTTATTTTGTAGCAGTAGAACAAATTAAAACAAACTATGGTGGAAAAGATTATAGTGG
401 AAAGGCAGTAGATCTACAGAAAATACGTGAAGAAGGGAAACGACAATACTTACCTAAAACATATACATTTGATGACGGATCAATTGTCTTCAAGACGGGA
501 GATAAAGTAACAGAAGAAAAAATTAAGAGATTATATTGGGCAGCCAAAGAAGTAAAAGCGCAATATCACCGTGTAATTGGTAATGATAAAGCACTAGAAC
601 CGGGTAACGCTGATGATGTACTAACAATAGTAATTTATAATAATCCAGATGAATATCAATTAAATAGACAATTATATGGATATGAAACAAACAACGGTGG
701 AAATTTATATTGAAAGAGAAGAGGGACCTTCTTTACATATGAGCGTACGCCAAAGCAGAGTATTTATAGTTTAGAGAAGTATTTCCCGTCATGGATCCCC
801 GTACATCGTTAGAAAGGCTTGCAATTCCGAAGCAGGAGAA
```

Figure 14. Sequencing of LV1 shows transposon insertion in B. anthracis genome. The genome of LV1 was BLASTed to compare with the *B. anthracis* genome. The sequence highlighted blue is homologous to the known transposon sequence.

```
  1 CTATCAGCACTGTTATCAACACCAGATCGTTACTGGGATTTCATGGTCCCCGTACATCGTTAGAAGCTTGAATTCGAGCAGAGTGGGAATCATTTGAAGG
101 TTGGTACTAGAAGCTTGATTCGAGCAGAGTGGGAATCATTTGAAGGTGGGTACTAGAAACTTGAATTCGAGCAGAGTGGGGAACTTTTGAAGGGTGGGAC
201 TAGAAACTTGATTTCGGGCAGAGTGGGAATCCTTTGTAAGTGGGGACTTAAATATTTTGTTCTTTGAAGCGTTTATTATTTTTTGGT
```

Figure 15. Sequencing of 11F11 shows transposon insertion in *B. anthracis* genome. The genome of 11F11 was BLASTed to compare with the *B. anthracis* genome. The sequence highlighted blue is homologous to the known transposon sequence.

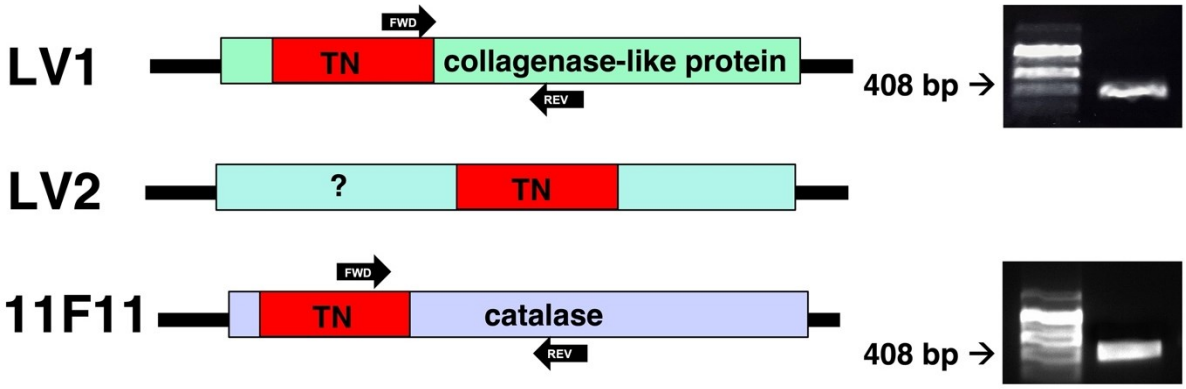

Figure 16. PCR confirmation of LV1 and 11F11. Left panel: Schematic of the transposon insertion and PCR confirmation using a transposon specific primer (black arrow labeled FWD) and a rev primer specific for each genomic region downstream of the transposon insertion (indicated by black arrow labeled REV). Right panel: Bands of expected size from the PCR reaction are shown.

DISCUSSION

Our objective was to identify mutants with increased susceptibility to hydrogen peroxide, and we identified two mutants, LV1 and LV2, out of approximately 1000 screened. Strangely, we observed a strong phenotype in the initial screen using 96-well plates but could not replicate the phenotype in LV2 a year later when performing the large-volume MIC assay using culture tubes. Growing our overnight cultures in a smaller volume in static conditions provides less aeration to the bacterium, providing less supply of necessary oxygen for cell growth. Growing our overnight cultures with more aeration could be promoting differential gene expression and therefore a change in phenotype in our large-volume MIC assay. Performing parallel assays using both methods moving forward will allow us to make a stronger conclusion for this fluctuation in the observed phenotype of LV1 and LV2.

Interestingly, this phenomenon was also observed with our *G. mellonella* survival assay. We saw a strong phenotype in our initial screen in the spring of 2022; however, when I went back to perform the assay again in the summer of 2022, I observed a weaker phenotype across the board for all mutants. Yet, this weaker phenotype also corresponded to a lower percent waxworm survival rate with our negative control, PBS. My hypothesis for this phenomenon is the varying age of waxworms used. Since these worms are outsourced from an online bait shop, we are unable to control for age-related factors like differences in the development of their immune systems. Therefore, an older worm could have a stronger immune response when injected with WT or the mutants. We are looking into breeding our own waxworms to control for age-related factors like this. While we recognize there are opportunities to use other models like *Caenorhabditis elegans,* we will continue troubleshooting with our *G. mellonella* model because there are distinct advantages to this invertebrate worm model. For example, we can precisely

know the amount of bacterium injected into each waxworm. The *C. elegans* are much smaller in size and therefore must be fed the bacterium– preventing us from knowing the number of bacteria ingested by the waxworms. We can also incubate *G. mellonella* at 37 ºC, which is a more relevant physiological temperature [15].

The 11F11 mutant had one of the strongest phenotypes in our H_2O_2 MIC assay and this phenotype made sense when we discovered that the gene disruption is in a gene encoding a catalase enzyme. Catalase has been previously characterized in *B. anthracis* and is known to be vital for the bacteria to cope with oxidative stress by converting hydrogen peroxide, a reactive oxygen species, to water and oxygen [18]. In LV1, it was interesting to discover that the site of insertion is in a gene encoding a collagenase-like protein. Bacterial collagenases have been linked to other bacterial strains as critical virulence factors [19] because of their ability to degrade collagen, the largest component in the extracellular matrix of animal cells. However, it remains unclear as to why this mutant was linked to increased hydrogen peroxide susceptibility. Collagenase has not been linked to scavenging reactive oxygen species yet; however, this enzyme may play a role in coping with oxidative stress that has not been studied yet.

To further confirm that this gene disruption is linked to the observed phenotype of LV1, I attempted to make an independent insertional mutant. I was able to successfully create my targeting vector and transform into all three bacterial strains; however, I was never able to successfully insert my vector into the bacterial genome at the region of homology I initially cloned into my vector. One reason for this issue could be that the region of homology we chose may not be compatible for plasmid integration. However, after all three of my attempts to put the plasmid under heat stress and force integration into the bacterial chromosome, I still had colonies grow on my erythromycin plates without successful integration into my region of homology. One

hypothesis for this acquired erythromycin resistance despite being grown at 37 °C could be that the plasmid acquired a mutation in the temperature sensitive origin of replication, and that plasmid persisted in the population. This would desensitize the plasmid to temperature-specific sensitivity at 30 °C and therefore allow the plasmid to continue replicating and erythromycin resistance to persist. Another plausible explanation could be that the plasmid inserted into another region in the bacterial chromosome where there were similarities in the region of homology cloned in. Both hypotheses allow our LV1 insertional mutant to gain erythromycin resistance while not disrupting the LV1-specific gene encoding a collagenase-like protein. Moving forward, we plan to consider creating a new targeting vector for LV1 by cloning in a new region of homology to get successful integration. Additionally, we will attempt to create a complement strain to restore the phenotype of LV1 and further verify the phenotype is linked to this gene disruption. We will also continue working towards identifying the transposon insertion site in LV2.

This research has successfully identified a novel chromosomal gene linked to virulence in *B. anthracis.* As we continue to live in a constantly evolving antibiotic resistance era, identifying novel drug therapeutic targets in the genome of *B. anthracis* is important so we can have alternative options to treat anthrax. While some bacterial infections are cleared by the rapid response of our immune system, others need the administration of antibiotics to help halt bacterial growth and proliferation. A new strategy called the anti-virulence strategy has surfaced in the field of antibiotic development where antibiotics are developed to disarm the bacteria in the host organism by inhibiting bacteria-specific mechanisms that promote infection and persistence within the host [20]. By targeting individual virulence mechanisms, rather than directly killing the bacteria, these anti-virulence therapeutics may have a decreased risk of

developing antibiotic resistance compared to traditional antibiotics [21]. With further characterization, this collagenase like protein could serve as a future antibiotic target in anthrax antivirulence treatment. Moreover, this antibiotic could be used to treat other bacterial infections if this collagenase-like protein is linked to virulence in other bacterial species. Staying ahead of antibiotic resistance by developing new antibiotics and alternative treatment options will help us combat entering an era of incurable, terminal bacterial illnesses.

REFERENCES

1. Moayeri, M., et al., *Anthrax Pathogenesis.* Annu Rev Microbiol, 2015. **69**: p. 185-208.
2. Spencer, R.C., *Bacillus anthracis.* J Clin Pathol, 2003. **56**(3): p. 182-7.
3. Jiranantasak, T., et al., *Characterization of Bacillus anthracis replication and persistence on environmental substrates associated with wildlife anthrax outbreaks.* PLoS One, 2022. **17**(9): p. e0274645.
4. Zasada, A.A., *Injectional anthrax in human: A new face of the old disease.* Adv Clin Exp Med, 2018. **27**(4): p. 553-558.
5. Sweeney, D.A., et al., *Anthrax infection.* Am J Respir Crit Care Med, 2011. **184**(12): p. 1333-41.
6. Dixon, T.C., et al., *Anthrax.* N Engl J Med, 1999. **341**(11): p. 815-26.
7. in *Review of the Scientific Approaches Used during the FBI's Investigation of the 2001 Anthrax Letters*. 2011: Washington (DC).
8. Read, T.D., et al., *The genome sequence of Bacillus anthracis Ames and comparison to closely related bacteria.* Nature, 2003. **423**(6935): p. 81-6.
9. McGillivray, S.M., et al., *ClpX Contributes to Innate Defense Peptide Resistance and Virulence Phenotypes of Bacillus anthracis.* Journal of Innate Immunity, 2009. **1**(5): p. 494-506.
10. Franks, S.E., et al., *Novel Role for the yceGH Tellurite Resistance Genes in the Pathogenesis of Bacillus anthracis.* Infection and Immunity, 2014. **82**(3): p. 1132-1140.
11. Purves, J., et al., *Comparison of the regulation, metabolic functions, and roles in virulence of the glyceraldehyde-3-phosphate dehydrogenase homologues gapA and gapB in Staphylococcus aureus.* Infect Immun, 2010. **78**(12): p. 5223-32.
12. Peleg, A.Y., et al., *Galleria mellonella as a model system to study Acinetobacter baumannii pathogenesis and therapeutics.* Antimicrob Agents Chemother, 2009. **53**(6): p. 2605-9.
13. Mylonakis, E., et al., *Galleria mellonella as a model system to study Cryptococcus neoformans pathogenesis.* Infect Immun, 2005. **73**(7): p. 3842-50.
14. Cotter, G., S. Doyle, and K. Kavanagh, *Development of an insect model for the in vivo pathogenicity testing of yeasts.* FEMS Immunol Med Microbiol, 2000. **27**(2): p. 163-9.
15. Malmquist, J.A., M.R. Rogan, and S.M. McGillivray, *Galleria mellonella as an Infection Model for Bacillus anthracis Sterne.* Frontiers in Cellular and Infection Microbiology, 2019. **9**.
16. Kwon, Y.M. and S.C. Ricke, *Efficient amplification of multiple transposon-flanking sequences.* J Microbiol Methods, 2000. **41**(3): p. 195-9.
17. Callaghan, L.T., *Discovering Novel Genes that Allow Bacillus anthracis to Survive Host Defenses*, in *Department of Biology*. 2020, Texas Christian University: Fort Worth, Texas. p. 32.
18. Rahi, A., et al., *Enzymatic characterization of Catalase from Bacillus anthracis and prediction of critical residues using information theoretic measure of Relative Entropy.* Biochem Biophys Res Commun, 2011. **411**(1): p. 88-95.

19. Kassegne, K., et al., *Identification of Collagenase as a Critical Virulence Factor for Invasiveness and Transmission of Pathogenic Leptospira Species.* Journal of Infectious Diseases, 2014. **209**(7): p. 1105-1115.
20. Cegelski, L., et al., *The biology and future prospects of antivirulence therapies.* Nat Rev Microbiol, 2008. **6**(1): p. 17-27.
21. Ford, C.A., I.M. Hurford, and J.E. Cassat, *Antivirulence Strategies for the Treatment of Staphylococcus aureus Infections: A Mini Review.* Front Microbiol, 2020. **11**: p. 632706.